COMPUTER SIMULATION OF NONLINEAR

ION-ELECTRON INSTABILITY

R.H. Berman, D.J. Tetreault, T.H. Dupree,
and
T. Boutros-Ghali

PFC/JA81-29

Computer Simulation

of Nonlinear

Ion-Electron Instability

R.H. Berman

D.J. Tetreault

T.H. Dupree and

T. Boutros-Ghali

Massachusetts Institute of Technology

Cambridge, MA 02139

ABSTRACT

An instability is observed whose onset occurs for electron drifts well below the threshold of the linear ion acoustic instability, and which, ultimately, dominates the nonlinear evolution of the linear instability. Detailed phase space diagnostics show that the fluctuations: (1) can be triggered by thermal level fluctuations; (2) occur over a broad velocity range including regions of large negative $\partial \langle f \rangle_{ion}/\partial v$; (3) have growth rates of the order of the trapping time; and (4) have dimensions that are typically a fraction of the thermal velocity and a few Debye lengths. The simulation results are consistent with the theoretical predictions of electron and ion clump regeneration. Although the simulation was one dimensional, similar phenomena theoretically are predicted to occur in three dimensional systems in the presence of a magnetic field and spatial density gradients. Therefore the simulations results have important implications for the role of linear theory, both in determining plasma stability and as a component of turbulence theory.

We report numerical experiments that show an instability well below the threshold predicted by linear theory. We studied a simulation plasma with mass ratio $m_i/m_e = 4$ and temperature ratio $T_e/T_i = 1$ in which, initially, the average electron distribution ($\langle f_e \rangle = (2\pi v_e^2)^{-1/2} \exp[-(v-v_d)^2/2v_e^2]$) drifts relative to the average ion distribution ($\langle f_i \rangle = (2\pi v_i^2)^{-1/2} \exp(-v^2/2v_i^2)$). According to linear theory such a plasma is unstable (the ion-acoustic instability for physical mass ratios) for drifts exceeding a certain threshold, $v_d = 3.924 v_i$. We observed an instability for $v_d \geq 1.5 v_i$.

For our simulations we used a highly optimized, one dimensional, electrostatic code with $N_p = 102,400$ particles per species. We treated a periodic system of length $L = 32.42\lambda_d$, where λ_d ($\equiv v_i/\omega_{p_i}$) is the Debye length and ω_{p_i} is the ion plasma frequency. Various diagnostics were performed which provide information about the fluctuations δf of the distribution function: $\delta f = f - \langle f \rangle$. For our spatially periodic and homogeneous system, the ensemble average $\langle \rangle$ was approximated by a spatial average. The two basic diagnostics we used were the mean square electric field and the mean square fluctuation $\langle \delta N^2 \rangle$ of the number of particles, N (electron or ion), in a phase space cell of size Δx, Δv. Here, $\delta N = N - \langle N \rangle$ where $\langle N \rangle$ is the mean number of particles in a cell. We would have preferred to measure the correlation function $\langle \delta f(1) \delta f(2) \rangle = \langle \delta f(x_1, v_1) \delta f(x_2, v_2) \rangle$ directly, for small $x_- = x_1 - x_2$ and small $v_- = v_1 - v_2$. Unfortunately, our value of $n_0\lambda_d = 3259.5$ ($n_0 = N_p/L$) was not large enough to provide adequate statistical accuracy. Our diagnostics, however, derive from the correlation function since the mean square electric field involves velocity integrals over $\langle \delta f \delta f \rangle$, while $\langle \delta N^2 \rangle$ and $\langle \delta f \delta f \rangle$ are related through[1]

$$\langle \delta N^2 \rangle = \left\langle \left(n_0 \int_x^{x+\Delta x} dx \int_v^{v+\Delta v} dv\, \delta f(x, v) \right)^2 \right\rangle$$
$$= n_0^2 \int_{-\Delta x}^{\Delta x} dx_- (\Delta x - |x_-|) \int_{-\Delta v}^{\Delta v} dv_- (\Delta v - |v_-|) \langle \delta f(1) \delta f(2) \rangle. \qquad (1)$$

Since $\langle \delta N^2 \rangle$ is a double integral of $\langle \delta f \delta f \rangle$, it is less sensitive to statistical error. The latter point is clearer when one realizes that Eq. (1) can be solved for the correlation function in terms of a fourth derivative of $\langle \delta N^2 \rangle$.

We can write, for each species,

$$\langle \delta f(1) \delta f(2) \rangle = n_0^{-1} \delta(x_-)\, \delta(v_-)\, \langle f(1) \rangle + g_d(1, 2) + g_v(1, 2), \qquad (2)$$

3

where the first term of Eq. (2) is the discrete particle self-correlation function and $g_d(1, 2)$ accounts for correlated fluctuations which shield the discrete particles. $g_v(1, 2)$ represents the effects of fluctuations over and above this level. Using the first term of Eq. (2) in Eq. (1), we find that the self-correlation contribution to $\langle \delta N^2 \rangle$ is $\langle N \rangle$—the value for randomly located discrete particles. This value is modified by the contribution from g_d; in particular, as the linear stability threshold is approached, the zeroes of the dielectric function will enhance $\langle \delta N^2 \rangle$ through the emmission and absorption of weakly damped waves. We have calculated[2] this contribution to $\langle \delta N^2 \rangle$ and have found it to be, consistently, much lower than the values of $\langle \delta N^2 \rangle$ observed in the simulations (cf. Fig. 1). Our observations of $\langle \delta N^2 \rangle$ are, therefore, evidence for collective fluctuations $g_v(1, 2)$ well above the dressed test particle level.

We measured $\langle \delta N^2 \rangle$ in cells of size $.05 v_i \leq \Delta v \leq 3 v_i$ by $.2 \lambda_d \leq \Delta x \leq 3 \lambda_d$. The characteristic sizes of the fluctuations in space $(\overline{\Delta x})$ and in velocity $(\overline{\Delta v})$ were inferred from the dependence of $\langle \delta N^2 \rangle / \langle N \rangle$ on Δx, Δv, given by Eq. (1). For Δx, Δv less than the characteristic size, $\langle \delta N^2 \rangle / \langle N \rangle$ increases with Δx, Δv since $\langle \delta N^2 \rangle \simeq n_0^2 \langle \delta f^2 \rangle (\Delta x \, \Delta v)^2$ and $\langle N \rangle = n_0 \langle f \rangle \Delta x \, \Delta v$. For Δx, Δv greater than the characteristic size, $\langle \delta N^2 \rangle \simeq n_0^2 \Delta x \, \Delta v \int_{-\infty}^{\infty} dx_- \int_{-\infty}^{\infty} dv_- \langle \delta f(1) \delta f(2) \rangle$ so that $\langle \delta N^2 \rangle / \langle N \rangle$ approaches a constant value. For $\Delta x < \overline{\Delta x}$, $\Delta v > \overline{\Delta v}$ and *vice versa*, $\langle \delta N^2 \rangle$ becomes proportional to Δx and Δv respectively. Fig. 2 is a typical plot of $\langle \delta N^2 \rangle / \langle N \rangle$, for the ions, versus cell size. It indicates that the ion fluctuation curves stopped increasing and turned over when $\Delta x \simeq 4 \lambda_d$ and $\Delta v \simeq .1 v_i$. Thus, these values of Δx and Δv represent the characteristic sizes $\overline{\Delta v}$ and $\overline{\Delta x}$.

Fig. 1 shows the time dependence of $\langle \delta N^2 \rangle / \langle N \rangle$ for the ions for a run with $v_d = 2.5 v_i$. After starting at unity, $\langle \delta N^2 \rangle / \langle N \rangle$ had risen by $\omega_{p_e} t = 150$ to the shielded discrete particle level, which we calculated to be 2.2. Subsequently, growth occurred until $\omega_{p_e} t = 300$. Following this unstable growth phase, the instability saturated when the electron distribution function formed a plateau in velocity space. We measured the fluctuation levels at $-v_i$, 0, v_i and $2 v_i$. Fluctuations with phase velocities of v_i and $2 v_i$ grew, while those at 0 and $-v_i$ decayed. This would seem to indicate that the instability grows in regions of opposing velocity gradients of $\langle f_e \rangle$ and $\langle f_i \rangle$. Furthermore, we note that the instability occurred in regions of large negative $\partial \langle f_i \rangle / \partial v \neq 0$—a region where linear

4

theory would predict strong damping of the fluctuations. Fig. 3 shows that the fluctuations are unstable over a wide region of velocity space ($0 \leq v \leq 4v_i$). This is evidenced by the ion tail and distorted electron distribution at $400\omega_{p_e}^{-1}$. These distortions in $\langle f_i \rangle$ and $\langle f_e \rangle$ are not the result of discrete particle collisions, since the collisional relaxation time is substantially larger than the run time of the simulation. Moreover, ion acoustic waves cannot be responsible, since, according to linear theory, they are stable.

Numerous runs were made to study various features of the instability: First, we examined the effect of using different initial conditions to start the simulation. These included: quite starts with $\langle \delta N^2 \rangle / \langle N \rangle \ll 1$; "thermal level" starts with $\langle \delta N^2 \rangle / \langle N \rangle \approx 1$; and "noisy" starts with $\langle \delta N^2 \rangle / \langle N \rangle \approx 4$. In all cases an instability was observed for $v_d \geq 1.5v_i$. Thus, to trigger the instability we did not require large amplitude fluctuations. In fact, the amplitude $\langle \delta N^2 \rangle / \langle N \rangle \simeq 1$ corresponds to $e\langle \phi^2 \rangle^{1/2} / m_i v_i^2 \simeq 10^{-2}$, where $\langle \phi^2 \rangle$ is the mean square potential.

Second, we investigated the dependence of the instability on v_d. Aside from the growth rate, there were no apparent qualitative differences between the runs for $1.5v_i \leq v_d \leq 4.5v_i$. After an initial growth stage, the instability saturated by forming a quasi-linear plateau. The ion distribution function developed a tail and the electron distribution function became significantly flattened as indicated in Fig. 3. We emphasize that these distortions were evident for v_d both below and above the linear stability threshold. The dependence of γ, the observed growth rate, on v_d is illustrated in Fig. 4. The measurements were made, for the ions, at approximately the same amplitude $\langle \delta N^2 \rangle / \langle N \rangle$ for each run (the electron $\langle \delta N^2 \rangle / \langle N \rangle$ gave similar growth rates). The error bars indicate the spread in the measured values of the growth rate when different methods were used to obtain γ. These methods consisted of measuring γ from the mean square electrostatic field, and from the time dependence of $\langle \delta N^2 \rangle / \langle N \rangle$ at different phase velocities ($v/v_i = .5, 1, 2$), and different cell sizes ($\Delta x / \lambda_d = 1, 2, \Delta v / v_i = .1, .2$). Also shown on Fig. 4 is the linear growth rate γ_L for the most unstable wavenumber. It is clear that the nonlinear effects dominated in the linearly unstable, as well as the linearly stable, region since $\gamma_L < \gamma$.

The third feature we examined was the effect of varying the parameter $n_0 \lambda_d$. When we

5

decreased $n_0 \lambda_d$ to 815, no change in γ occurred. From this, we concluded that discrete particle collisions, apparently, did not play an important role. Below the nonlinear threshold, we saw the fluctuations decay. For $v_d = 0$, we measured the same decay rate observed in a series of one species calculations with $n_0 \lambda_d = 65, 190$ reported elsewhere[3].

The measured characteristics of the instability are consistent with the non-linear theory of ion and electron "clump" regeneration[4]. In a Vlasov plasma, clumps result from the mixing of the incompressible phase space density by turbulent fluctuations[5,6]. If the clump production rate is equal to their destruction rate (through velocity streaming and the turbulent electric fields) the clump spectrum will regenerate. Overregeneration implies an instability. In Ref. 4 it was theoretically predicted, for the parameters of this simulation, that a clump spectrum would regenerate in regions of opposing velocity gradients for $v_d \geq 2.5 v_i$. In addition, the spectrum would exhibit a wide phase velocity spread (c. the order of v_i) and characteristic scales $(\overline{\Delta x}, \overline{\Delta v})$ similar to those observed in this simulation. Moreover, approximate calculations[7] show that for a mass ratio of 4, the clump instability has an amplitude dependent growth rate proportional to the inverse ion trapping time $(\tau_{tr} \equiv \overline{\Delta x}/\overline{\Delta v})$. The constant of proportionality (which is of the order of unity) increases rapidly with v_d and $-\partial \langle f_e \rangle / \partial v \partial \langle f_i \rangle / \partial v$. The observed values of $\overline{\Delta x}$ and $\overline{\Delta v}$ lead to a trapping time of the order of $80 \omega_{p_e}^{-1}$ which is consistent with the measured growth rates (cf. Fig 4).

The existing calculations of clump regeneration omit a number of terms that describe the effects of self-binding of the fluctuations. Clumps are enhancements ($\delta f \geq 0$) or depletions ($\delta f \leq 0$) in the local phase space density . The depletions, or "holes", have the property of being self-binding[8]. Such an effect would decrease the destruction rate of the fluctuations and therefore reduce the predicted drift velocity threshold. This would also be consistent with the slow (about $0.1 \tau_{tr}^{-1}$) decay rate observed at $v_d = 0$. It is interesting to note that a single, isolated phase space hole has been shown to be unstable for all $v_d > 0$[9]. This isolated hole instability is driven by opposing velocity gradients of $\langle f_i \rangle$ and $\langle f_e \rangle$ and is the analogue to the turbulent clump instability.

Although the nonlinear instability discussed in this Letter is one dimensional and driven by velocity gradients, we believe that it is representative of an important new class of instabilities

6

since clump and hole phenomena are predicted to occur in three dimensions with a magnetic field. For instance, it has recently been shown that a single phase space hole in a magnetic field is unstable to a spatial density gradient[9]. This result implies that the clump instability will be driven by a spatial density gradient. Furthermore, our simulation indicates that large amplitudes are not necessary for its onset. Indeed, we have observed the instability growing out of thermal level fluctuations.

References

[1]T. H. Dupree, C. E. Wagner and W. M. Manheimer, *Phys. of Fluids*, 18, 1167 (1975).

[2]The calculation is for the case Δx, $\Delta v > \overline{\Delta x}$, $\overline{\Delta v}$. For smaller size windows $\langle \delta N^2 \rangle$ would be smaller.

[3]R. H. Berman, D. J. Tetreault and T. H. Dupree, *Bull. Amer. Phys. Soc.*, 25, 1035 (1980); *Proc. Ninth Conf. on Numerical Simulation of Plasmas*, Chicago, to be published (1980).

[4]T. Boutros-Ghali and T. H. Dupree, "Theory of Nonlinear Ion-Electron Instability", MIT Plasma Fusion Center, Report No. PFC/JA-81-6, (1981), submitted to *Phys. of Fluids*.

[5]T. H. Dupree, *Phys. of Fluids*, 15, 334 (1972).

[6]T. Boutros-Ghali and T. H. Dupree, *Phys. of Fluids*, 24, 1839 (1981).

[7]D. J. Tetreault, "Growth rate of the Clump Instability," MIT Plasma Fusion Center, report No. PFC/JA-81-25 (1981).

[8]T. H. Dupree, *Phys. of Fluids*, 27 (1982).

[9]T. H. Dupree, *Bull. Amer. Phys. Soc.*, 26, 1060 (1981).

Figure Captions

Figure 1. Ion $\langle \delta N^2 \rangle / \langle N \rangle$ for a phase space cell of dimensions $\Delta x = 1.963\lambda_d$, $\Delta v = .1 v_i$ versus time for $v_d = 2.5 v_i$. The points are the simulation values measured at different velocities $(\times) - 1v_i$; $(+)0v_i$; $(*)v_i$; and $(O)2v_i$. The dashed line is the shielded discrete test particle level.

Figure 2. Ion $\langle \delta N^2 \rangle / \langle N \rangle$ for a phase space cell of dimensions Δx, Δv. The points are the simulation values: $(+)$ $\langle \delta N^2 \rangle / \langle N \rangle$ vs. $20\Delta v/v_i$ at fixed $\Delta x = .98\lambda_d$; $(\times)$ $\langle \delta N^2 \rangle / \langle N \rangle$ vs $\Delta x/\lambda_d$ at fixed $\Delta v = .1 v_i$.

Figure 3. The spatially averaged distribution functions for the ions and electrons for $v_d = 2.5 v_i$ at $\omega_{p_e} t = 400$ (solid curve) and at 0 (dashed curve).

Figure 4. The simulation values of the growth rate γ versus the electron drift v_d. $(+)$ denote single measurements while the error bars include several measurements. The growth rate γ_L obtained from linear stability theory is also plotted.
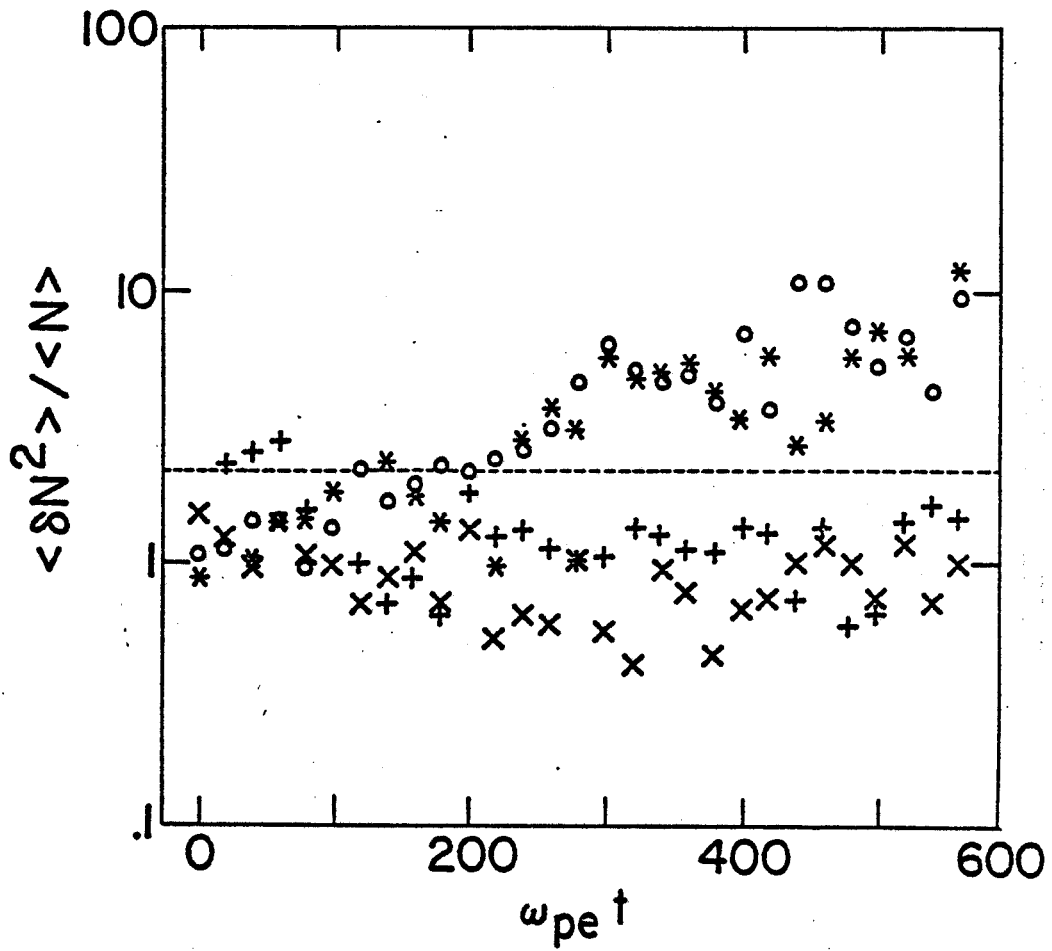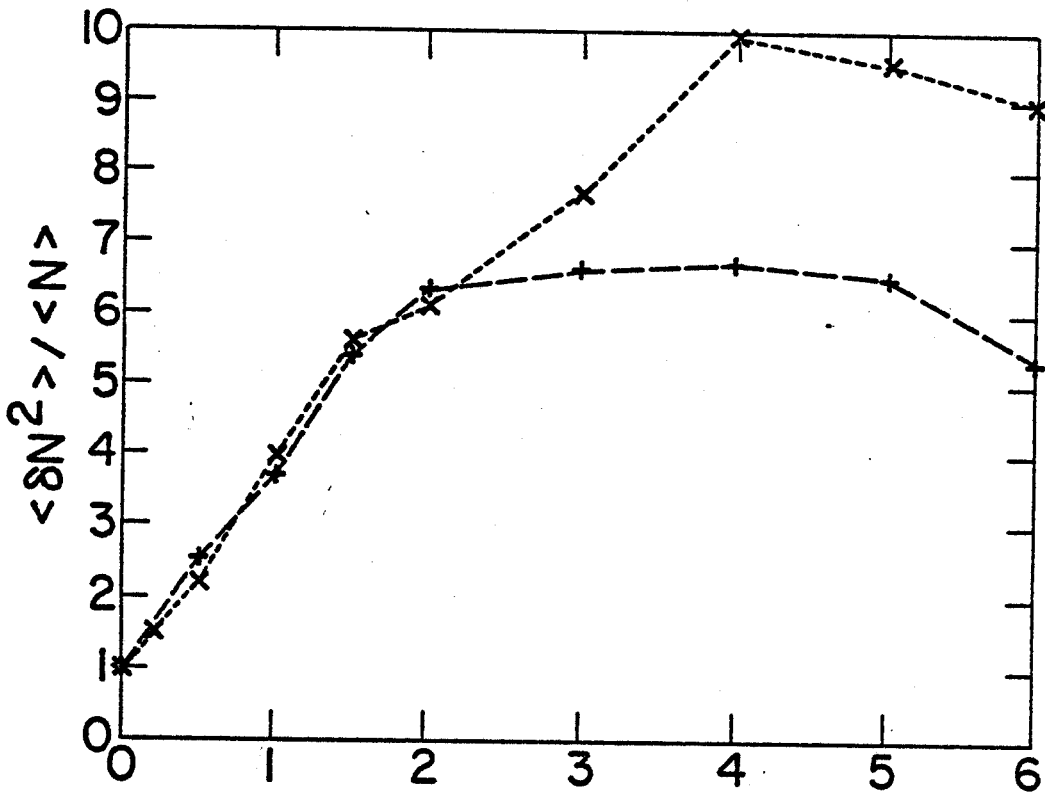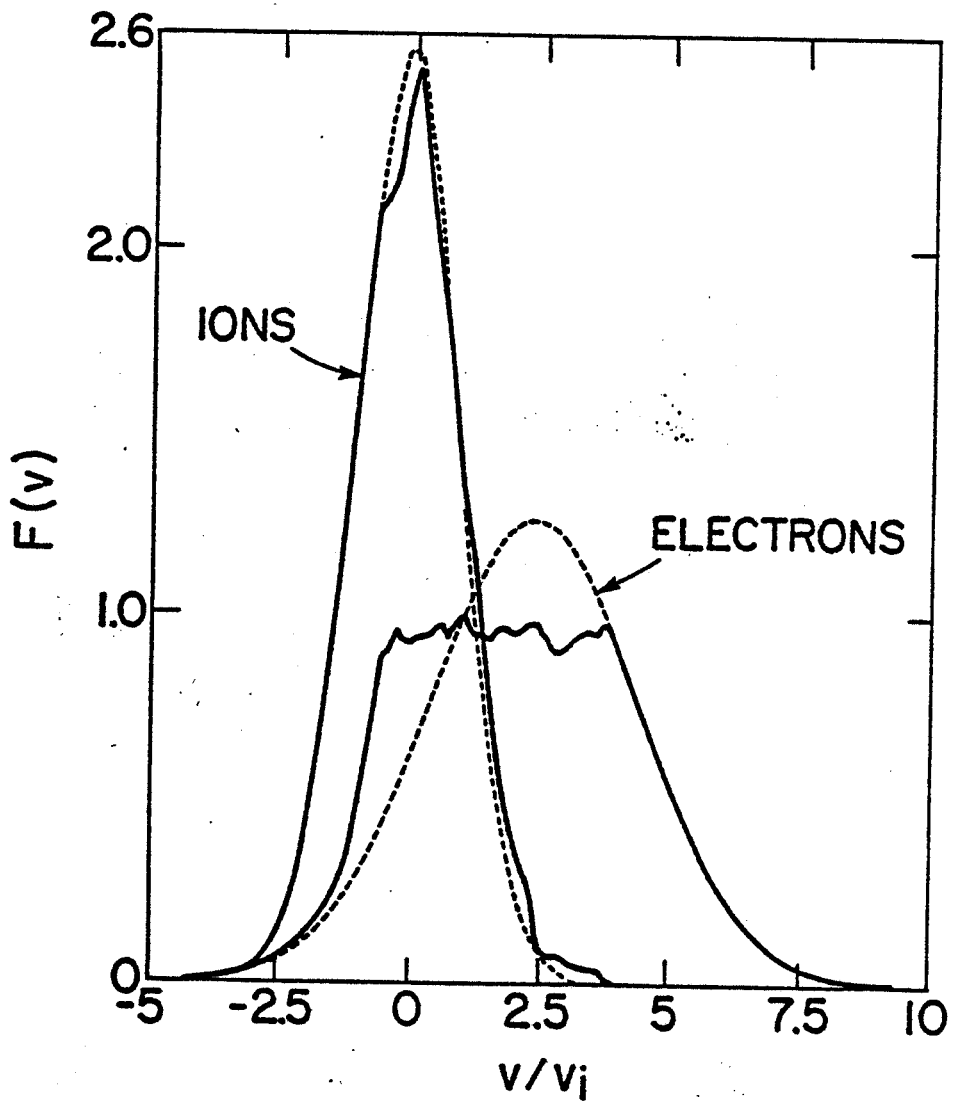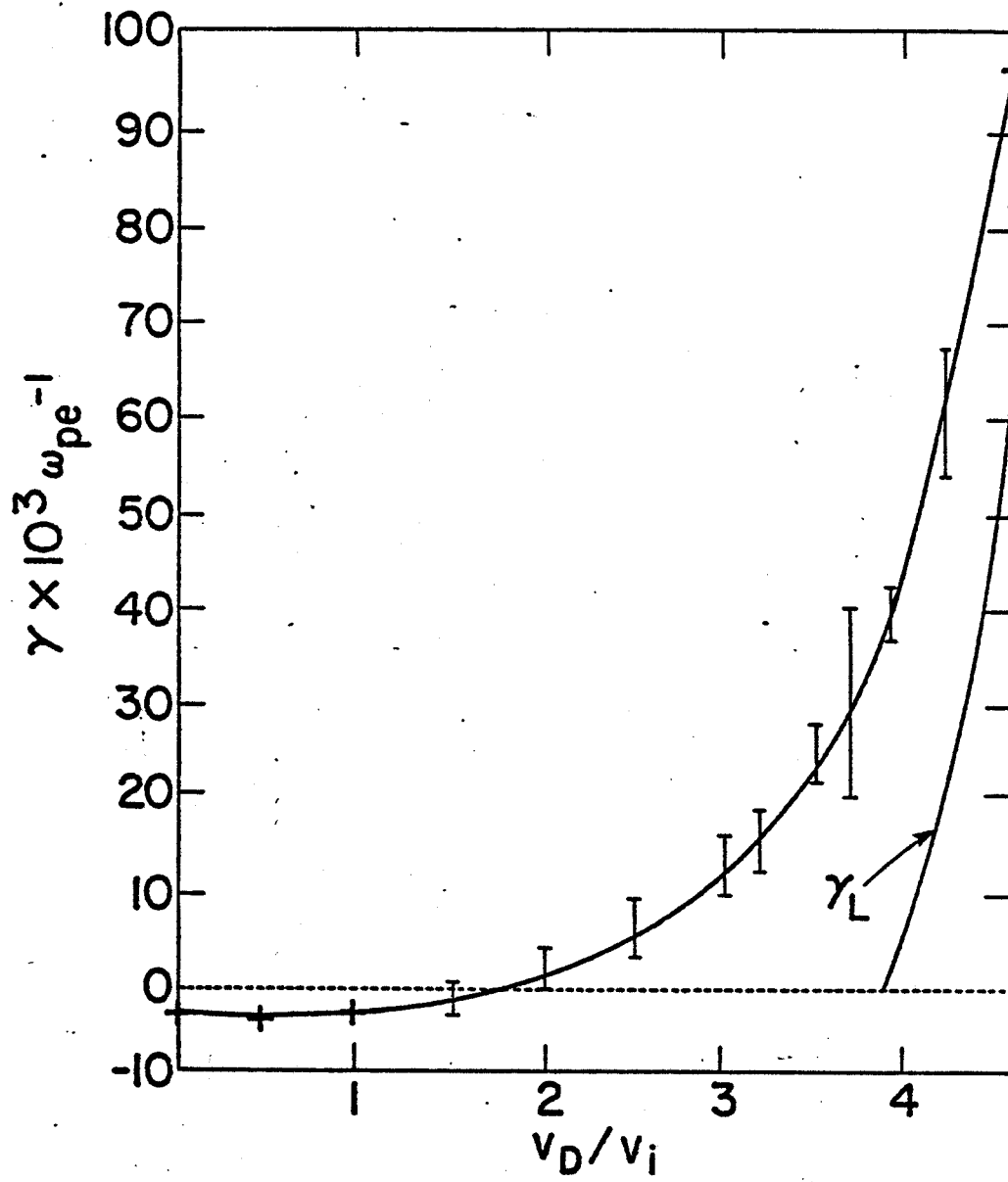
FIGURE 1

FIGURE 2

FIGURE 3

FIGURE.4